PAPER

Check for updates

Thermodynamically leveraged solventless aerobic deconstruction of polyethylene-terephthalate plastics over a single-site molybdenum-dioxo catalyst†

Naveen Malik,[a,b] Jiaqi Li,[a] Amol Agarwal,[c] Yosi Kratish ✱[a] and Tobin J. Marks ✱[a]

Here, we describe the solventless catalytic deconstruction of polyethylene-terephthalate (PET) under an aerobic atmosphere, mediated by an earth-abundant, low-cost activated carbon (AC)-supported single-site molybdenum-dioxo catalyst (AC/MoO$_2$). Catalytic amounts of AC/MoO$_2$ selectively convert waste PET into its monomer, terephthalic acid (TPA), within 4 h at 265 °C with yields as high as 94% under 1 atm air. Pure crystalline TPA product sublimes from the reaction hot zone, crystallizing on the reactor cold zone, thus avoiding the need for separation and purification steps. This process does not employ any hazardous/toxic reducing agents or solvents, and the catalyst can be recycled multiple times without loss of activity, rendering this process highly atom-efficient. According to computational and experimental mechanistic studies, the AC/MoO$_2$ catalyst mediates a thermoneutral metal-catalyzed β-scission step, followed by an exothermic step that converts the vinyl benzoate intermediate to TPA and acetaldehyde using trace amounts of moisture in the air. The formation of gaseous acetaldehyde makes the isolation of TPA from the reaction mixture facile and industrially favorable, especially since solvents are unnecessary. The present methodology is also extended to the deconstruction of other frequently used polyester plastics, polybutylene terephthalate (PBT), polyethylene naphthalate (PEN), and polyethylene furanoate (PEF), and operates equally well with post-consumer waste products. Notably, this process is also compatible with plastic mixtures of polyesters with polyolefins, polyamides, and polycarbonates, leading to the selective conversion of each polyester to the corresponding monomer, leaving the residual polymer unchanged and polyester-free.

Green foundation

1. Polyethylene terephthalate (PET) is a widely used plastic with annual production >70 million tons. In 2021, only 29% of post-consumer PET in the US was recycled, with most waste ending up in landfills due to costly collection and sorting. Chemical recycling by catalytic deconstruction offers a viable alternative to recover monomers, but traditional methods are often non-sustainable. Here we present a new solvent-free, rapid PET depolymerization process using trace moisture from ambient air, catalyzed by a recoverable carbon-supported single-site molybdenum-dioxo catalyst.

2. This approach avoids the formation of waste salts and high-boiling byproducts common in conventional hydrolysis approaches, making it environmentally benign and green.

3. This process is compatible with various post-consumer wastes and plastics mixtures, offering a green strategy to address the global plastic waste challenge while inspiring chemists to develop alternative solutions for sustainable plastic recycling.

---

[a]*Department of Chemistry, Northwestern University, Evanston, Illinois 60208, USA.*
E-mail: yosi.kratish@northwestern.edu, t-marks@northwestern.edu
[b]*Department of Chemistry, College of Engineering and Technology, SRM Institute of Science and Technology, Kattankulathur, Tamil Nadu 603203, India*
[c]*Department of Materials Science and Engineering, Trienens Institute for Sustainability and Energy, Northwestern University, Evanston, Illinois 60208, USA*
†Electronic supplementary information (ESI) available. See DOI: https://doi.org/10.1039/d4gc05916f

Introduction

Plastics find extensive global applications in diverse industrial products owing to their light weight, exceptional durability, and cost-effectiveness. This over-dependency on plastic products, fueled by societal lifestyle changes, has significantly enhanced their economic importance.[1–3] It is esti-

mated that approximately 8300 megatonnes (Mt) of plastic have been produced since the 1950s, with the demand for plastics escalating from 2 Mt per year to 368 Mt per year in the last seven decades, with predictions forecasting a quadrupling of this demand by 2050.[4-6] According to a 2018 US Environmental Protection Agency (EPA) study, 35.7 million tons of plastic garbage were produced in the US, accounting for 12.2% of all municipal solid waste.[7,8] In addition to polyethylene terephthalate (PET) bottles, this waste material also includes polyethylene (PE), and polypropylene (PP) as bags, wraps, automotive parts, construction materials, bottles, *etc*.[9] Based on European data, the EU produced approximately 34.4 kg of plastic packaging waste per resident in 2019. However, only around 14.1 kg, equivalent to 41% of that waste, is recycled, indicating a significant gap between production and recycling rates and contributing to the accumulation of plastic in the environment.[10,11] The poor biodegradability of commonly used plastics and the widespread use of monomers derived from fossil fuels in plastics manufacture presents a significant environmental concern. Plastics don't readily degrade but accumulate in natural environments and landfills, leading to persistent pollution. Plastic waste is notorious for infiltrating major oceanic expanses, contaminating freshwater ecosystems, and degrading terrestrial habitats over time.[7,12] The destiny of the millions of tons of plastics that evade recycling is either incineration or landfill disposal, leading to an estimated annual economic loss of $80–120 billion worldwide. According to one estimate from a US EPA report, by recovering and recycling just packaging plastic such as PP, PET, *etc*., the US could have saved 81.5 trillion Btu in energy in 2015. This value is equivalent to two million households' annual electricity consumption. According to a recent US EPA report, a tonne of recycled plastic could save 30 cubic yards of landfill space, 16.3 barrels of oil, and 98 million Btus of energy.[8,12]

PET has emerged as an essential engineering plastic due to its high optical transparency, excellent chemical stability, barrier properties, and mechanical characteristics. Currently, PET finds widespread application in the production of plastic films, electronic devices, fibers, beverage bottles, mechanical equipment, food packaging, and various other fields, with annual production worldwide reaching nearly 70 million tons.[9] Based on information from Euromonitor International (London, England), PET bottles dominate the beverage industry, commanding 67% of the market share. Notably, PET packaging constituted 44.7% of the single-serve beverage packaging market in the US in 2021, compared to aluminum cans (39%) and glass (11%).[13,14] However, PET contributes ≈ 12% of global solid waste, and excessive use with low recycling rates has led to its accumulation in landfills and ecosystems, posing environmental hazards to human health and wildlife. Moreover, its reliance on fossil feedstocks highlights the need for advanced recycling methods to mitigate resource depletion.[15-25] Notably, each ton of PET containers manufactured from recycled plastic would reduce energy consumption by ≈7200 kW h and CO_2 emissions by ≈5.1 tons.[13]

Nowadays, the most common method to recycle end-of-life polyester products is thermo-mechanical recycling, in which sorted plastic is washed, shredded, and remelted.[26] While this method is economically favorable, it is highly dependent on the quality and cleanliness of the sorted plastics, producing, in many cases, inconsistent quality of downcycled plastic with limited application. For this reason, most polyester plastic waste streams are considered non-recyclable, leading to low polyester recycling rates. To address this issue, alternative methods such as enzymatic and chemical recycling are being investigated to degrade PET into one or more monomers, offering potential solutions for recycling.[15-25,27-31] Various approaches such as glycolysis,[32-34,57] alcoholysis,[35,36] hydrogenolysis/hydrolysis,[37-46] and aminolysis[47,48] are under investigation (Scheme 1, top A–D). Non-catalyzed processes typically require substantial amounts of alcohols or water, extended reaction times (up to 72 h), high temperatures (250–400 °C), pressure (1–35 MPa), and acidic or alkaline conditions.[37-46] Additionally, the production of oligomers and the necessity to separate the desired monomers from the reaction mixture detract from the efficiency of these methods. Moreover, in most cases, clean, sorted polyester feedstocks in the form of PET bottles are still required for efficient chemical recycling. To increase reaction rates and moderate reaction conditions, homogeneous metal-based catalysts are typically employed in these processes.[49,50] In some cases, ionic liquids and deep-eutectic solvents are also used.[51,52] However, these methods still face the same limitations, including adverse environmental impact of the reaction solvents, challenging monomer separation from the side products, reaction solvent and catalysts. Furthermore, due to the challenges in recovering the soluble metal catalysts, most catalysts used are single-use or disposable, generating additional quantities of waste and posing environmental challenges.

To address the catalyst recovery concern, heterogeneous catalysts can be employed since they can be simply filtered at the end of the reaction. Several heterogeneous catalysts (zeolites and various nanocatalysts) have been recently reported to mediate PET depolymerization, mostly using significant amounts of solvents in methanolysis, glycolysis, and aminolysis.[33,53-61] Among these, metal oxide catalysts have been widely used due to their unique chemical and/or magnetic properties or ease of catalyst recovery. Thus, Kim reported the use of separable super-paramagnetic γ-Fe_2O_3 as a catalyst for PET chemical recycling by glycolysis.[56] Rinaldi reported a cobalt nanoparticle-based heterogeneous catalyst for the depolymerization of PET by glycolysis.[57] Other notable examples include shape-engineered manganese oxide (MnO_x) nanocatalysts, micronsized MgO-coated SiO_2 catalysts, magnetically recyclable $CoFe_2O_4$ nanocatalysts, and nanostructured Nb_2O_5 materials have been reported for PET glycolysis and aminolysis.[58-61] The use of harsh reaction conditions, solvents, difficulty in separating monomers from the reaction mixture, poor product selectivity, and prolonged reaction times remain unsolved challenges.[53-61] Additionally, developing cost-effective catalysts made from earth-abundant metals is essen-

tial for the industrialization of such processes. To the best of our knowledge, no heterogeneous catalysts have emerged for PET degradation under solvent-free conditions using trace amounts of moisture. Further literature survey reveals that, to date, only a handful of reports are available for the selective deconstruction of PET (using heterogeneous catalysts) in a mixture of plastics.[62,63] Thus, the need to develop a green, solvent-free, atom-efficient process with a reusable, cheap, non-toxic catalyst that can deconstruct neat polyesters or those admixed with other plastics under mild conditions remains highly desired.

Recently, we reported on the efficacy of an earth-abundant carbon-supported (AC = activated carbon) single-site molybdenum-dioxo catalyst (AC/MoO_2) to deconstruct PET to terephthalic acid (TPA) and ethylene in the presence of 1 atm of H_2.[64] Although, this process is solvent-free and produces readily isolated pure crystalline TPA, the long reaction time (24 h) and use of hazardous H_2 gas introduce significant drawbacks. In addition, the compatibility of this process with mixed plastic waste streams was barely investigated. Therefore, in this report, we describe a significantly more efficient approach to produce TPA from PET in the presence of ambient air, using catalytic amounts of AC/MoO_2. Quantitative conversions of PET to TPA are achieved within 4 h at 265 °C, which is PET's melting temperature; moreover, the process is also operative at 250 °C (Scheme 1, bottom i). The catalysis does not require hazardous reducing agents, is solvent-free, and can be recycled multiple times without deactivation, making this process extremely safe and atom-efficient. Moreover, it will be seen that this process is compatible with a variety of other commodity polyesters, such as polybutylene terephthalate (PBT), polyethylene naphthalate (PEN), and polyethylene furanoate (PEF), producing the corresponding dicarboxylic acid monomers (Scheme 1, bottom ii).

In addition, this process functions equally well with end-of-life post-consumer polyester products such as bottles, shirts, pillow stuffings, and plumbing supplies. Finally, note that this process is also efficient in dealing with common mixed commodity plastic polyester waste streams, including those containing polyolefins, polycarbonates, and polyamides (Scheme 1, bottom iii). Experimental kinetic and theoretical studies suggest that the AC/MoO_2 catalyst facilitates a thermoneutral metal-catalyzed β-scission step of PET, followed by a strongly exothermic step that converts the vinyl benzoate intermediate to TPA and acetaldehyde in the presence of humid air. To the best of our knowledge, this is the first report of a solvent-free chemical recycling process for polyesters using trace amounts of moisture from the air.

Results and discussion

To establish an environmentally friendly methodology for the solventless deconstruction of polyesters, initial studies included optimization of reaction parameters such as reaction time, temperature, catalyst support, and metal center effects on PET deconstruction. The reaction was first carried out using PET and AC/MoO_2 mixtures under solvent-free conditions at 265 °C. Heating the PET and AC/MoO_2 mixture in a 100 mL Schlenk reaction flask under ambient air (relative humidity ≈ 26%) resulted in formation of the desired TPA monomer (1) as a solid polycrystalline product (Table 1 and Fig. S1†). Initially, the ester : Mo mole ratio was held at 26 : 1, and reactions were carried out for different time intervals (Table 1, entries 1–4 and Fig. S2–S5†). TPA was obtained in 68% yield within 2 h of heating (Table 1, entry 1), and happily, an 88% yield of TPA is formed after 4 h (Table 1, entry 2). Extending the reaction time to 6 h and 24 h does not increase the yield further, as indicated in Table 1, entries 3 and 4. Not surprisingly, due to mass transfer limitations given the PET melting point of 260 °C, rates are sluggish below this temperature, as evidenced by the 30% yield of TPA obtained after heating the reaction at 250 °C for 4 h (Table 1, entry 5 and Fig. S6†). Increasing the reaction temperature to 280 °C resulted in an 81% TPA yield after 4 h (Table 1, entry 6 and Fig. S7†). Remarkably, decreasing the catalyst loading to a 34 : 1 ester : Mo mole ratio increased the TPA yield to 93% on heating for 4 h at 265 °C (Table 1, entry 7 and Fig. S8†). However, further decreasing the ester : Mo mole ratio to 45 : 1, 54 : 1 and 110 : 1 produced moderate yields of TPA of 79%, 51% and 49%, respectively (Table 1, entries 8–10 and Fig. S9–S11†), verifying that the catalyst plays a crucial role in accelerating the reaction kinetics.

The TPA product formation was confirmed by a distinct aromatic singlet of aryl proton (H1) at 8.04 ppm in the ^1H NMR spectrum (Fig. S8†). By expanding the y-scale of the ^1H NMR spectrum and integrating, we conclude that the purity of TPA is ≥97%. Similarly, the ^{13}C NMR spectrum exhibits three characteristic peaks at chemical shifts of 129.9, 134.9, and 167.1 ppm, corresponding to the aromatic (C3), quaternary aromatic (C2), and carbonyl carbons (C1) of TPA, respectively (Fig. S8†). No other impurity peaks and ethylene glycol moiety (aside from those arising from the NMR solvent) are detected. The NMR spectra (^1H and ^{13}C) indicate high purity of recovered TPA and are in excellent agreement with previously reported TPA NMR data.[64–66]

To test possible metal effects on PET depolymerization while keeping all other variables such as support (= activated carbon) and reaction conditions constant, we investigated AC/WO_2 where the literature data suggests that the tungsten dioxo has weaker electron-accepting capacity.[67,68,81] Employing a similar synthetic approach to that of AC/MoO_2, the analogous single-site AC/WO_2 catalyst was synthesized (see Experimental section for details). However, changing the metal center to WO_2 was less fruitful, and only 10% yield of TPA monomer was obtained under the optimized conditions (Table 1, entry 11, and Fig. S12†). Overall, the higher activity of MoO_2 in PET deconstruction compared to WO_2 can be attributed to its superior electron-accepting capacity and stronger interaction with the ester substrate, which likely affords higher catalytic activity.[67,68,81] The reaction in the absence of MoO_2, i.e., activated carbon (AC), resulted in minimal TPA formation with 6% yield (Table 1, entry 12 and Fig. S13†), arguing that the AC

Conventional Catalytic PET Degradation Processes

A. PET Transesterification for recycling

PET + ROH →[Catalyst] + HO‑CH₂CH₂‑OH (b.p. 197 °C)

❖ Low efficiency
❖ Large excess solvents
❖ Product separation tedious
❖ Oligomers side products
❖ High boiling inseparable product

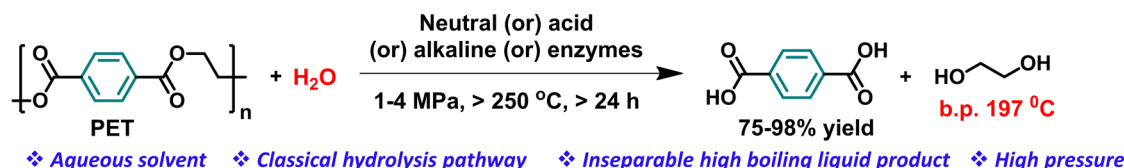## B. PET degradation to BHET or BHETA *via* glycolysis or aminolysis

PET + HO‑CH₂CH₂‑OH or H₂N‑CH₂CH₂‑OH →[Catalyst]
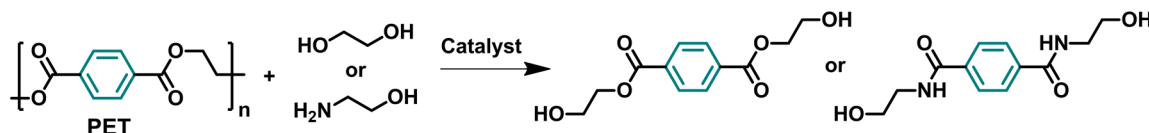
❖ Organic solvents ❖ Poor solubility of PET in solution ❖ Oligomers side products ❖ Non-environmental sustainability

C. PET hydrogenative degradation to diols

PET + H₂ →[[Ru] or [Mn] Catalyst, > 50 bar] + HO‑CH₂CH₂‑OH (b.p. 197 °C)
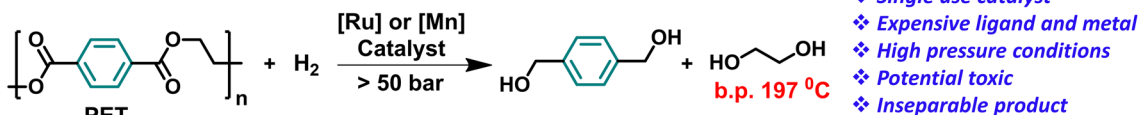
❖ Single use catalyst
❖ Expensive ligand and metal
❖ High pressure conditions
❖ Potential toxic
❖ Inseparable product

## D. PET depolymerization to TPA and ethylene glycol *via* classical hydrolysis

PET + H₂O →[Neutral (or) acid (or) alkaline (or) enzymes; 1-4 MPa, > 250 °C, > 24 h] TPA (75-98% yield) + HO‑CH₂CH₂‑OH (b.p. 197 °C)

❖ Aqueous solvent ❖ Classical hydrolysis pathway ❖ Inseparable high boiling liquid product ❖ High pressure

This Work: Unconventional Aerobic PET Deconstruction

(i) Depolymerization of PET to TPA and acetaldehyde *via* non-classical pathway

PET + Moist Air →[AC/MoO₂; 1 atm, 265 °C, 4 h] TPA (up to 94% yield) + acetaldehyde (gas) [AC/MoO₂]
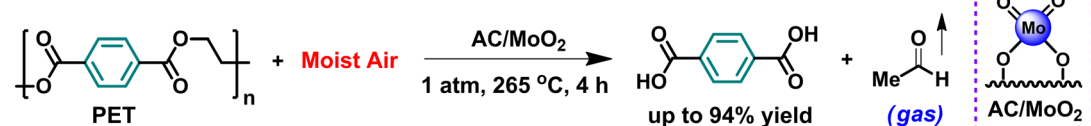
❖ Solvent-free ❖ Moist air mediated non-classical hydrolysis ❖ Low catalyst loading ❖ Recyclable low cost catalyst
❖ Low pressure conditions ❖ Easy product/co-product isolation ❖ Sustainable pathway ❖ Post-consumer plastics

(ii) Polyester scope: Depolymerization of diverse polyesters to monomers

PBT or PEN or PEF
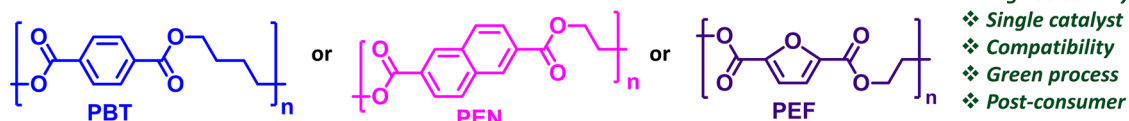
❖ High selectivity
❖ Single catalyst
❖ Compatibility
❖ Green process
❖ Post-consumer

(iii) Mixed plastics: Selective polyester depolymerization

PC, PET, i-PP, PBT, Nylon-6 →[AC/MoO₂] TPA →[Separation] i-PP, PC, Nylon-6
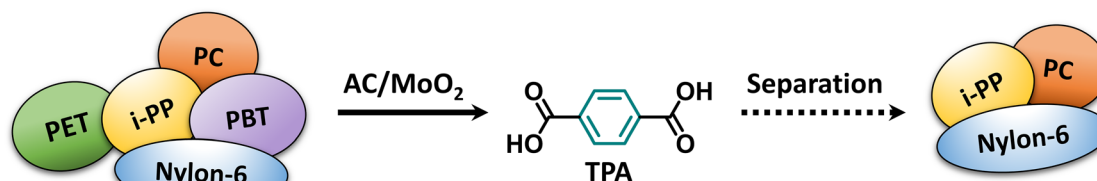
Scheme 1 (Top and Bottom) Comparison of polyethylene terephthalate (PET) chemical recycling pathways and applicability to other polyesters.
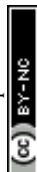
Table 1 Optimization of catalytic conditions for the depolymerization of polyethylene terephthalate (PET)

Entry	Gas	t [h]	T [°C]	Catalyst	Ester/Mo [mol]	TPA yield (%)
1	Air	2	265	AC/MoO$_2$	26 : 1	68
2	Air	4	265	AC/MoO$_2$	26 : 1	88
3	Air	6	265	AC/MoO$_2$	26 : 1	87
4	Air	24	265	AC/MoO$_2$	26 : 1	85
5	Air	4	250	AC/MoO$_2$	26 : 1	30
6	Air	4	280	AC/MoO$_2$	26 : 1	81
7	**Air**	**4**	**265**	**AC/MoO$_2$**	**34 : 1**	**93**
8	Air	4	265	AC/MoO$_2$	45 : 1	79
9	Air	4	265	AC/MoO$_2$	54 : 1	51
10	Air	4	265	AC/MoO$_2$	110 : 1	49
11	Air	4	265	AC/WO$_2$	34 : 1	10
12	Air	4	265	AC	—^{a}	6
13	Air	4	265	—	—	11^b
14	Air	4	265	CNH/MoO$_2$	34 : 1	32
15	Air	4	265	AlS/MoO$_2$	34 : 1	45
16	Argon	4	265	AC/MoO$_2$	34 : 1	2,^{c} n.d.^{d}
17	Vac	4	265	AC/MoO$_2$	34 : 1	n.d.,^{e} 90^f
18	Water	4	265	AC/MoO$_2$	34 : 1	20^g
19	Air	20	265	AC/MoO$_2$	170 : 1	94 (83)^h

General reaction conditions: 100 mL Schlenk reaction flask, PET stored in air, catalysts, solventless, air, 2–24 h. Terephthalic acid (TPA, **1**) yields calculated by ^{1}H NMR using mesitylene as internal standard. ^{a} 32 mg of activated carbon (AC) used. ^{b} PET heated in the absence of AC/MoO$_2$. ^{c} Air stored PET and AC/MoO$_2$ charged in reaction flask. Flask sealed in argon-filled glove box. ^{d} Vacuum-dried PET and AC/MoO$_2$ charged in the reaction flask. Flask sealed in argon-filled glove box. Negligible product formed; see ESI† for more details. n.d. = not determined. ^{e} Air stored PET and AC/MoO$_2$ charged in a reaction flask, and flask sealed under a static vacuum of 10^{-6} Torr. Negligible product formed, see ESI† for more details. n.d. = not determined. ^{f} Air stored PET and AC/MoO$_2$ first heated under vacuum for 4 h followed by heating under air for 4 h; see ESI† for more details. ^{g} Air stored PET and AC/MoO$_2$ heated in the presence of 10 μL water (3× excess *vs.* the PET repeat unit) without air; for more experimental details see ESI. ^{h} Fresh PET added after every 4 h of reaction. Isolated yields of TPA in parenthesis. CNH = carbon nanohorn, AlS = sulfonated alumina and Vac = vacuum.

surface is not significantly involved in the catalytic process and highlighting the catalytic importance of the MoO$_2$ center. In the absence of AC/MoO$_2$ or AC, the reaction yielded 11% TPA monomer, providing additional evidence for the catalytic role of MoO$_2$ in PET deconstruction (Table 1, entry 13 and Fig. S14†).

To further understand the role of the support in PET degradation, "super-acidic" sulfonated alumina (AIS) and carbon nanohorn (CNH) supports were used to support MoO$_2$ catalysts.[69,70] When CNH/MoO$_2$ catalyst was used, only 32% yield of TPA was obtained (Table 1, entry 14 and Fig. S15†). Although CNHs have many unique properties, such as high dispersibility, electron transparency, and large surface area, CNH is a delicate single-layer support that might be prone to damage under oxidative reaction conditions, such as heating at high temperatures under air. In contrast, AC is thermally

more robust and retains its structural integrity and functionality even under such harsh conditions. In the case of AlS/MoO$_2$, a 45% TPA yield was obtained (Table 1, entry 15 and Fig. S16†), suggesting that the super acidic nature of the support is less crucial for PET deconstruction.

After obtaining optimized conditions for PET deconstruction, attention was turned to investigating the role of moisture in this process and the fate of the expected ethylene glycol (EG) moiety. Water can enter the reaction flask through two primary sources: (i) ambient air and (ii) physisorbed water from the air-stored PET and AC/MoO$_2$. Two control reactions were first conducted under an inert atmosphere to test for the latter. Thus, air-stored PET and AC/MoO$_2$, were placed in a flask filled with argon gas and heated for 4 h at 265 °C. This produced TPA in 2% yield (Table 1, entry 16 and Fig. S17†). When this reaction was repeated using vacuum-dried PET and AC/MoO$_2$, no TPA was detected (Table 1, entry 16). Consequently, these experiments support the critical role of ambient moisture in the PET deconstruction process. Clearly, the moisture inherent in PET and in the AC/MoO$_2$ catalyst is insufficient to facilitate catalytic PET deconstruction under the present conditions. To further probe the impact of atmospheric air on PET, an additional control experiment was performed. Specifically, heating the PET and AC/MoO$_2$ catalyst mixture in a degassed reaction flask under 10^{-6} Torr vacuum conditions yielded negligible amounts of TPA monomer (Table 1, entry 17 and Fig. S18†). Interestingly, exposing the same reaction mixture to ambient air for 8 min and subsequently continuing the reaction under air for another 4 h, significantly enhanced PET conversion, providing a 90% TPA yield, and highlighting once more the importance of moisture on the reaction outcome and showing that AC/MoO$_2$ is thermally stable and does not deactivate upon heating (Fig. S18 and S19†).

To demonstrate the impact of a more moisture-laden atmosphere on PET depolymerization, we replaced ambient air with water droplets in the reaction flask. Interestingly, heating PET with 10 μL of water (3× excess *vs.* the PET repeat unit) under standard vacuum conditions affords only a 20% TPA yield (Table 1, entry 18 and Fig. S20†). The lower TPA yield with excess water is tentatively attributed to a side reaction in which H$_2$O adds to the Mo=O bond in tetra-coordinated AC/MoO$_2$ to yield a sterically more hindered penta-coordinated AC/Mo(=O)(OH)$_2$ intermediate which may be less active in ester-activation reactions (*vide infra*). These results highlight the delicate balance of moisture that drives the reaction. Hence, atmospheric moisture, particularly from ambient air, emerges as a critical factor in the PET deconstruction dynamics and even a 3× (*vs.* the PET repeat unit) excess of moisture in the reaction flask significantly slows the PET depolymerization.

In the next phase, we evaluated the catalyst's durability and suitability for a continuous depolymerization process (Fig. 1). This is an essential test of a sustainable plastic recycling process. Thus, one can envision an industrial process in which PET is continuously introduced to the catalyst in the reaction setup while volatile TPA is continuously produced. To simulate a continuous process, a multi-batch depolymerization experi-

Fig. 1 The photographs show the TPA product formation at different runs after every 4 h of heating (total reaction time = 20 h).

ment was conducted with a low catalyst loading (ester : Mo ratio of 170 : 1). A fresh PET charge was introduced into the reaction flask every 4 h for a total of five additions. This approach yielded an overall depolymerization efficiency of 94% (Table 1, entry 19, Fig. 1 and Fig. S21†), indicating that the catalyst maintains high activity with negligible deactivation, likely reflecting its thermal stability. To determine whether the single-site molybdenum center remains structurally intact under these reaction conditions, we performed X-ray photoelectron spectroscopy (XPS) on both fresh and spent catalysts. The XPS analysis showed identical Mo $3d_{5/2}$ orbital peak at 232.7 eV in both samples, indicating that the single-site Mo(vi) catalyst remains chemically stable and recyclable after multiple reaction cycles (Fig. S22†). This experiment conclusively establishes the durability of the catalyst and it's suitability for a continuous process.

In the next stage, we sought to understand how AC/MoO$_2$ catalyzes PET deconstruction. In a classical PET hydrolysis scenario, one would expect to obtain EG together with TPA (Scheme 2).[44–46] Surprisingly, neither EG nor its derivatives are detected by NMR spectroscopy in DMSO-d_6 as the solvent, suggesting that the catalysis is operating *via* a different mechanism (Fig. S2–S21†). Interestingly, monitoring the headspace gases after PET deconstruction using FTIR spectroscopy revealed the presence of acetaldehyde (a gas at 25 °C), explain-

ing why TPA is the only detectable product in the NMR spectra (Fig. S23–S26†). In addition, when the headspace gas was collected and dissolved in D$_2$O, acetaldehyde, and its cyclic oligomer 1,3,5-trioxane, 2,4,6-trimethyl were identified (Fig. S27†). Note that this catalyst is also known to be a good aldehyde oligomerization catalyst, and the formation of the cyclic trimer was reported previously.[64,71,72]

Based on the present observations and previous work,[64] we hypothesize that the AC/MoO$_2$ first catalyzes the almost thermoneutral β-scission step (ΔG° = 1.2 kcal mol^{-1}), yielding a carboxylic acid and vinyl benzoate intermediates, followed by a strongly exergonic step (ΔG° = −17.7 kcal mol^{-1}) in which the vinyl benzoate intermediate is converted to a carboxylic acid and acetaldehyde in the presence of moisture (Scheme 2A). The overall Gibbs free energy for this pathway is −16.4 kcal mol^{-1} (Scheme 2A). Interestingly, for the classical stepwise hydrolysis pathway that produces carboxylic acids and EG, the first and second steps are computed to be almost isoneutral with Gibbs free energies of −0.1 kcal mol^{-1} and −1.8 kcal mol^{-1}, respectively, yielding an overall energy of −1.9 kcal mol^{-1} for this pathway (Scheme 2B). The fact that the classical hydrolysis pathway is 14.5 kcal mol^{-1} energetically disfavored is in good agreement with the experimental data shown in Table 1, *i.e.* acetaldehyde is observed with no EG detected (Fig. 2A).
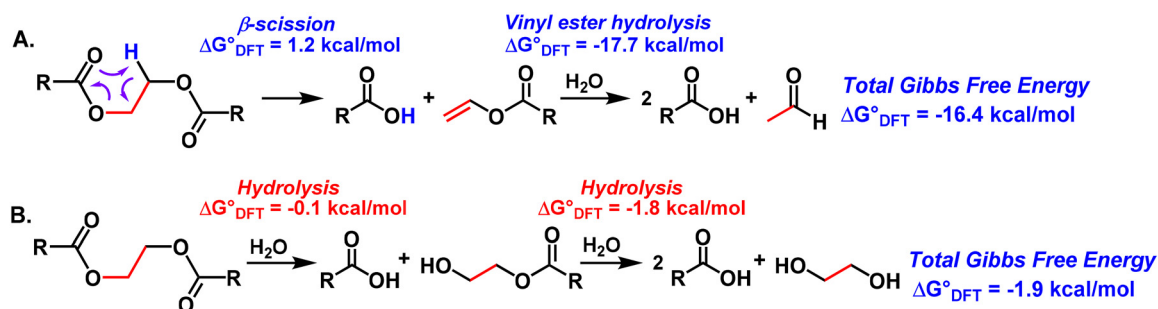
Scheme 2 Density functional theory (DFT)-computed polyester deconstruction pathways. R = Ph in computational studies.
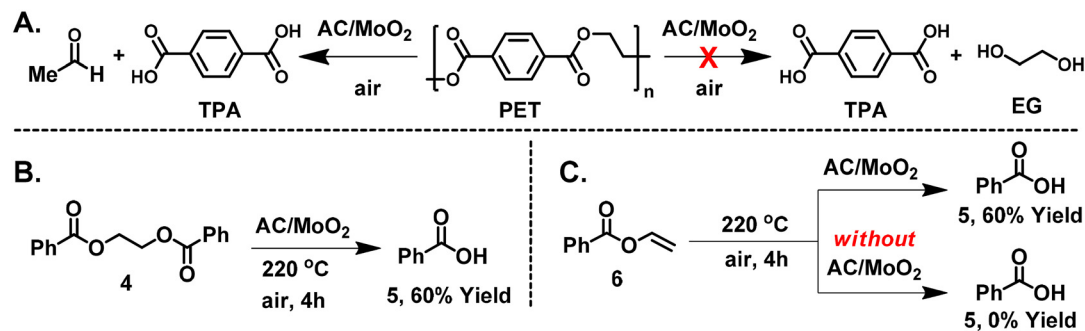
Fig. 2 (A) Expected hydrolysis products of PET depolymerization. (B and C) Control experiments with 1,2-ethanediol dibenzoate (**4**) and vinyl benzoate (**6**).

To further validate the pathway shown in Scheme 2A and to simplify the mechanistic analysis, several control experiments with ethane-1,2-diyl dibenzoate (**4**) and vinyl benzoate (**6**) were carried out (Fig. 2B and C). Due to the high volatility of **4**, the reaction was carried out at a lower temperature, 220 °C.[64,73] Pleasingly, **4** produces a similar reaction outcome, yielding colorless benzoic acid (**5**) crystals and acetaldehyde in 60% yield (Fig. 2B and Fig. S28, S31†). The lower yield is attributed to the lower reaction temperature, and even at 220 °C, some of **4** distills away from the reaction hot zone. To support the hypothesis that vinyl intermediates play a role in the catalysis, we conducted several control experiments with neat vinyl benzoate (**6**). Thus, when **6** is heated in the presence of AC/MoO₂, a 60% yield of benzoic acid (**5**) is obtained (Fig. 2C and Fig. S29†). However, in the absence of AC/MoO₂, **6** is fully recovered, and negligible benzoic acid (**5**) is obtained (Fig. 2C and Fig. S30†).

The control experiment results support the proposed pathway shown in Scheme 2. However, to gain a deeper understanding of the reaction mechanism, we conducted a detailed computational study using Density Functional Theory (DFT). To reduce computational costs, a simplified model diester, ethylene glycol diacetate, was chosen. The computational model of the single-site AC/MoO₂ catalyst shown in Fig. 3 has been validated in numerous prior mechanistic studies, demonstrating its reliability as a model system. The DFT calculations were performed at the CAM-B3LYP/Def2-SVP//CAM-B3LYP-D3/Def2-TZVP level of theory using the ORCA 4.1.0 package.[74]

The most probable reaction mechanism is depicted in Fig. 3A, with key transition states shown in Fig. 3B and the calculated energy profile illustrated in Fig. 3C. In the first step, the diester undergoes a β-scission reaction catalyzed by AC/MoO₂ (**A**) *via* a concerted six-membered ring transition state (**TS1**, Fig. 3B) to afford a carboxylic acid product and a Mo-coordinated vinyl ester intermediate **B** (Fig. 3A, step i). This step is slightly endothermic (3.1 kcal mol⁻¹), and **TS1** represents the rate-determining transition state with an energy barrier of 35.0 kcal mol⁻¹ (Fig. 3B and C). Isotopic labeling experiments further support this step, indicating that the carboxylic hydrogen atom (highlighted in purple in Fig. 3A) originates from the hydrogen attached to the glycol moiety.[64]

In the next step, a water molecule reacts with the Mo=O bond to form the dihydroxy species **C** (Fig. 3A, step ii). This reaction is slightly endothermic (5.6 kcal mol⁻¹) with a low transition state (**TS2**) barrier of 10.8 kcal mol⁻¹ (Fig. 3B and C). The O–H addition of water or alcohol molecules to the Mo=O bond in AC/MoO₂ has been previously reported, and the reaction proceeds readily under the present conditions.[75] However, excess water can inhibit the β-scission step by increasing the coordination number of the Mo center from four to five or six, thereby slowing the reaction rate (Table 1, entry 18 and Fig. S20†). Thus, maintaining an appropriate water concentration is critical for optimal reaction efficiency.

Next, an intramolecular nucleophilic attack of the hydroxide on the ester carbonyl forms an alkoxy intermediate **D** (Fig. 3A, step iii) in a mildly exothermic step (−4.2 kcal mol⁻¹) *via* transition state **TS3**, which has a barrier of 19.1 kcal mol⁻¹ (Fig. 3B and C).[64,76] Subsequently, in a concerted eight-membered ring transition state (**TS4**, Fig. 3B), the hydroxyl hydrogen migrates to the terminal carbon of the olefin, generating acetaldehyde and intermediate **E**. This step is exothermic (−6.8 kcal mol⁻¹) with a transition state barrier of 18.4 kcal mol⁻¹ (Fig. 3B and C). Finally, the second carboxylic acid product dissociates from intermediate **E**, regenerating the AC/MoO₂ catalyst (Fig. 3A, step v).

Alternative mechanisms, such as the hydrolysis of the vinyl ester in intermediate **C** to produce a carboxylic acid followed by acetaldehyde formation, were also explored computationally. However, these pathways were deemed less likely due to significantly higher energy barriers (by 6.5 kcal mol⁻¹; see Fig. S49† for more details).

Encouraged by the excellent catalytic activity demonstrated by AC/MoO₂ in deconstructing commercial PET plastics as powders, we extended this methodology to test post-consumer plastics such as beverage bottles, polyester shirts, and pillow stuffing. Impressively, 92%, 92%, and 93% TPA yields are obtained for the respective waste materials (Table 2, entries 2–4, Fig. 4A–C and Fig. S32–S34†), identical to the results obtained with pristine PET powder (Table 1, entry 7 and Table 2, entry 1). These results indicate a minimal influence of processing or stabilizing plastic additives on the catalytic process and underscore the potential of this solventless methodology. Subsequently, the
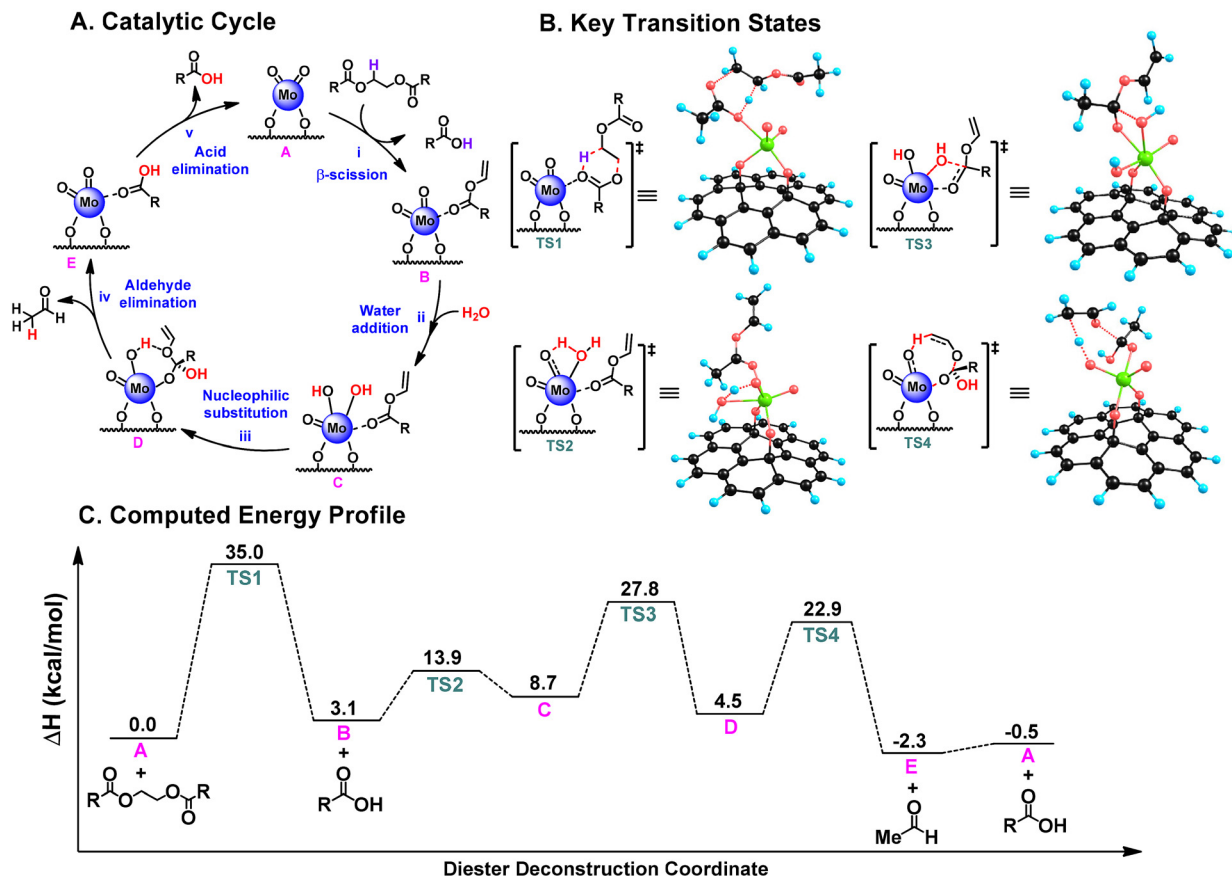
A. Catalytic Cycle

B. Key Transition States

C. Computed Energy Profile

Fig. 3 DFT analysis of diester deconstruction catalyzed by AC/MoO$_2$. (A) Computed catalytic cycle. (B) Key transition states. Green = molybdenum, black = carbon, red = oxygen, light blue = hydrogen (C) computed enthalpy profile in kcal mol^{-1}. R = Me in computational studies.

Table 2 Aerobic solventless AC/MoO$_2$-mediated depolymerization data for the indicated polyesters neat and admixed with other high-volume polymers

Entry	Polyester	t [h]	TPA yield (%)
1	PET (commercial)	4	93
2	PET (bottle)	4	92
3	PET (shirt)	4	92
4	PET (pillow)	6	93
5	PBT (commercial)	24	94, 4.4,[a] 88[b]
6	PBT (tube fitting)	24	82
7	PEN (commercial)	24	50[c]
8	PEF (powder)	3	40
9	PET + PC	10	82[d]
10	PET + i-PP	4	90[d]
11	PET + Nylon-6	4	80[e]
12	PET + PBT	24	90[d]

General reaction conditions: 100 mL Schlenk flask, polyester stored in air, AC/MoO$_2$ (3.24 wt% Mo), solventless, 265 °C in air. Product yield determined by ^{1}H NMR spectroscopy using mesitylene internal standard. [a] Air-stored PBT and AC/MoO$_2$ heated under argon. [b] Air stored PBT and AC/MoO$_2$ first heated under vacuum for 24 h followed by heating in air for 24 h, see ESI† for details. [c] Reaction at 290 °C. [d] 1:1 mixtures of PET/PC, PET/i-PP and PET/PBT plastics. Yield corresponds to TPA. [e] A 1:0.5 mixture of PET/Nylon-6 was used. Yield corresponds to TPA.

Fig. 4 Aerobic solventless AC/MoO$_2$-mediated deconstruction of post-consumer plastic materials A–D. Reaction conditions: 100 mL Schlenk flask, post-consumer polyester stored in air, AC/MoO$_2$ (3.24 wt% Mo), solventless, 265 °C, air. Yield determined by ^{1}H NMR using mesitylene internal standard.

catalytic applicability to other polyester plastics, PBT, PEN, and PEF (Table 2, entries 5–8, Fig. 4D and Fig. S35–S41†) was investigated. Using the solventless protocol described above with reaction temperatures elevated to the respective melting/softening points of these polyesters, it was found that PBT deconstructs to TPA in 94% yield, albeit at a lower rate than PET, necessitating a

24 h reaction time for full conversion at 265 °C (Table 2, entry 5 and Fig. S35†). In the absence of air, only a 4.4% TPA yield is obtained after 24 h, while the introduction of air to the reaction mixture affords an 88% TPA yield (Table 2, entry 5 and Fig. S36–S38†), demonstrating the positive influence of air on PBT conversion and confirming AC/MoO$_2$ stability at 265 °C over 48 h. Next, post-consumer waste black-colored PBT chips from tube fittings were subjected to identical reaction conditions (Table 2, entry 6, Fig. 4D). Here, colorless solid monomer sublimes to the flask top, illustrating the efficacy in processing challenging post-consumer plastic waste PBT plastics (Fig. S39†). Similarly, PEN and PEF undergo deconstruction to the corresponding monomers naphthalene dicarboxylic acid (50% yield) and 2,5-furan dicarboxylic acid (40% yield), respectively (Table 2, entries 7, 8 and Fig. S40, S41†).

Recycling mixed plastics is challenging due to the diverse physical properties of different plastics.[62,63,77–79] Post-consumer mixed plastics require sorting and separation before recycling, which is complex, expensive, and labor-intensive. Without proper pre-sorting, deconstruction becomes inefficient and nonselective, resulting in complex product mixtures with undesirable properties, and potential catalyst deactivation.[77–79] In principle, catalytic deconstruction might separate valuable products or desired monomers from plastics mixtures, but only a few catalysts or recycling technologies currently exist that can effectively and selectively deal with mixed plastics.[80] Here, we recover pure TPA from PET which is admixed with several other commodity plastics utilizing the AC/MoO$_2$ catalytic system.

To evaluate the scope of such separations, the following mixed plastics were examined: (i) PET + poly(bisphenol A carbonate (PC)), (ii) PET + isotactic-polypropylene (i-PP), (iii) PET + Nylon-6, and (iv) PET + PBT (Table 2, entries 9–12). Note that the presence of PC, PP, or Nylon-6 does not hinder the PET conversion performance; both high activity and selectivity in PET degradation are observed. Thus, heating a PET + PC mixture (1 : 1 molar ratio) at 265 °C affects the selective breakdown of PET to TPA (82% yield), with the PC remaining unchanged and recoverable from the reaction flask (Table 2, entry 9 and Fig. S42†). Furthermore, for a typical waste plastics mixture, such as PET + i-PP (a water bottle + cap plastic) in a 1 : 1 molar ratio, TPA sublimes out in 90% yield (Table 2, entry 10 and Fig. S44†). The i-PP remains in the reactor, unaffected by the reaction. Furthermore, heating a PET + Nylon-6 mixture in 1 : 0.5 molar ratio results in the selective deconstruction of PET to TPA in 80% yield (Table 2, entry 11, and Fig. S46†). Note that the presence of an amide linkage-based polymer does not hinder the PET degradative performance; both high activity and selectivity occur in PET depolymerization in the presence of Nylon-6.

The remarkably high selectivity towards PET deconstruction in mixtures with PC, i-PP, or Nylon-6 imbues a "catalytic separation" function to the present chemical recycling process. These results suggest that the operational parameters employed here do not promote significant scission of PC carbonate bonds, i-PP C–C bonds, or Nylon-6 amide bonds. For example, competing PC depolymerization would yield bisphenol A, which should be detectable by NMR; however, no such signals were observed

(Fig. S42 and S43†). Similarly, competing depolymerization of Nylon-6 would produce ε-caprolactam, which was also absent in the NMR spectra (Fig. S46 and S47†). Control experiments were performed by heating PC and Nylon-6 only under the same experimental conditions and no depolymerization products were detected in either case (Fig. S43 and S47†). In the PET/i-PP reaction, since i-PP depolymerization would be expected to yield gaseous products, the residue from the reaction flask was dissolved in CD$_2$Cl$_4$, confirming that i-PP remained unreacted in the reaction flask (Fig. S45†).[64] Nevertheless, the present reaction conditions are adequate to selectively break PET ester bonds. The chemical structure and purity of TPA recovered from the mixed plastics wastes were assessed by comparing ^{1}H NMR spectra (Fig. S42, S44 and S46†). In all cases, the ^{1}H NMR spectra reveal a singlet (8.04 ppm) corresponding to the aromatic protons of the TPA phenylene ring. Apart from the peaks corresponding to DMSO-d_6 (2.50 ppm) and H$_2$O (3.38 ppm), no other significant signals were detected in the ^{1}H NMR spectra. In the case of the PET + PBT mixture, TPA was formed through the degradation of PET and PBT plastics, resulting in a total TPA yield of 90% (Table 2, entry 12 and Fig. S48†). These findings highlight the robustness and versatility of the present catalytic method to address the challenge of mixed plastics recycling, offering promising strategies for sustainable waste management.

Conclusions

This work demonstrates the first example of aerobic PET deconstruction without solvents or a complex hydrolysis process. We show that a carbon-supported single-site molybdenum-dioxo catalyst mediates PET deconstruction under atmospheric conditions near the polymer melting temperature. The present methodology offers an alternative to environmentally harmful alkaline or acidic hydrolysis conditions traditionally employed for PET deconstruction with excess water as solvent under high temperatures and pressures.[44–46] Traditional acidic and alkaline hydrolysis processes generate substantial amounts of environmentally undesirable waste salts and/or water. The present approach enables the separation of pure TPA monomer from the reaction hot zone by condensation on the cooler reactor surfaces. This eliminates the need for additional steps to separate and purify the TPA, which are typically required in hydrolysis processes. Furthermore, typical hydrolysis processes have additional challenges, such as the energetics of separating ethylene glycol (EG) from water and ultimately disposing of the water. The present solventless process for polyester recycling is far more atom- and energy-efficient, and the low-cost catalyst is readily recycled. A detailed experimental and DFT mechanistic studies elucidated that the PET degradation mediated by metal-catalyzed (= AC/MoO$_2$) thermoneutral β-scission step of PET followed by a strongly exothermic step that converts the vinyl benzoate intermediate to TPA and acetaldehyde in the presence of humid air.

Interestingly, the presence of polypropylene (PP), Nylon-6, and polycarbonate (PC), common plastics mixtures, does not

affect the degradation of PET. The process has been used to degrade other polyesters and post-consumer products to obtain the corresponding monomers TPA (from PET and PBT), naphthalene dicarboxylic acid (from PEN), and 2,5 furandicarboxylic acid (from PEF) selectively. The method was also used to deconstruct common PET post-consumer waste, such as water bottles, pillow stuffing, and shirts. Notably, the use of black PBT plastic tube fittings affords colorless TPA products; therefore, the formation of significant discolored degradation products is not observed. We believe the present catalytic process is renewable, less toxic, and cheaper than current methods, making it safer, green and more sustainable for achieving a circular polyester plastic economy.

Experimental section

Material and methods

All manipulations of reagents were carried out in oven-dried reaction vessels unless otherwise noted. The reactions of all polyesters, 1,2-ethanediol dibenzoate (**4**), vinyl benzoate (**6**), were carried out in cylindrical 100 mL Schlenk vessels under air with heating supplied by a metal block (Fig. S1†). Schlenk vessels was purchased from Chemglass Life Sciences. Polyethylene terephthalate (PET) powder was purchased from Goodfellow Inc. with a specified particle size of 300 μm and containing 1 ppm of acetaldehyde. Polybutylene terephthalate (PBT) pellets, polyethylene naphthalate (PEN), poly(bisphenol A carbonate (PC, average MW ≈ 45 000)), and isotactic-polypropylene (*i*-PP) pellets were purchased from Sigma-Aldrich. Reagents, $CDCl_3$, DMSO-d_6, mesitylene were purchased from Sigma-Aldrich and used without further purification. Vinyl benzoate (**6**) and 1,2-ethanediol dibenzoate (**4**) were purchased from Sigma-Aldrich. AC/MoO$_2$, CNH/MoO$_2$ and AIS/MoO$_2$ were prepared and characterized previously by this group from (dme)MoO$_2$Cl$_2$ (dme = 1,2-dimethoxyethane).[64,69,70–72] AC/WO$_2$ was prepared by reaction of AC + (dme)WO$_2$Cl$_2$ using earlier reported procedure.[81] The loading of the Mo (3.24 wt%) and W (2.8 wt%) on carbon was determined by ICP analysis.

Physical and analytical measurements

NMR spectra were recorded on a Varian Bruker Avance III HD system equipped with a TXO Prodigy probe (500 MHz) spectrometer. Chemical shifts (δ) for ^{1}H are referenced to solvent resonances. Mesitylene was used as the internal standard. FTIR spectra of gaseous products were recorded on a Nicolet iS50 FTIR spectrometer equipped with an MCT detector and collected using a custom-built airtight gas cell (100 mm long, *ca.* 3 ml cell volume) with IR-transparent ZnSe windows. The detector was cooled with liquid N$_2$. A spectral resolution of 4 cm^{-1} was used, and the reported spectra are an average of 64 scans. For the FTIR measurements, the gas cell was first evacuated down to 100 mTorr, where a background spectrum was collected. In a typical experiment, a 5 ml charge of the sample was introduced to the cell *via* an injection port fitted with a silicon septum using an airtight syringe. Sample spectra were

collected against the background spectrum obtained under the vacuum. X-ray photoelectron spectroscopy spectra were recorded at the Keck-II facility at Northwestern University with a Thermo Scientific ESCALAB 250 Xi spectrometer, equipped with an Al K alpha radiation source and electron flood-gun, at a pressure of 8×10^{-8} mbar with a pass energy of 50 eV. Typically, a 50 ms dwell time and 10 scans were used for each spectrum. All spectra were calibrated according to the asymmetric graphitic peak at 284.8 eV using the Thermo Avantage software. Inductively coupled plasma (ICP) analysis was performed at the Northwestern University Quantitative Bioelement Imaging Center.

General procedure for polyester depolymerization

In a typical experiment, polyester, AC/MoO$_2$ (3.24 wt% Mo catalyst), and a PTFE-coated magnetic stir bar were added to a 100 mL J-Young reaction flask in open air (= lab condition). The reactor was then closed and heated in an aluminum block heater while stirring at 450 rpm (Fig. S1†). During the reaction, the products sublime from the reaction zone and crystallize near the top of the reaction tube (Fig. S1†). The conversion and selectivity were assayed by ^{1}H-NMR spectroscopy using integration against a mesitylene internal standard.

Data availability

The authors confirm that the data supporting the finding of this study are available within the article [and/or] its ESI.†

Conflicts of interest

There are no conflicts to declare.

Acknowledgements

References

1 I. Vollmer, M. J. F. Jenks, M. C. P. Roelands, R. J. White, T. van Harmelen, P. de Wild, G. P. van der Laan, F. Meirer, J. T. F. Keurentjes and B. M. Weckhuysen, *Angew. Chem., Int. Ed.*, 2020, **59**, 15402–15423.

2 S. George, in *Plastic Waste and Recycling*, ed. T. M. Letcher, Academic Press, New York, 2020, ch. 17, pp. 449–466.

3 J.-P. Lange, *ACS Sustainable Chem. Eng.*, 2021, **9**, 15722–15738.

4 J. R. Jambeck, R. Geyer, C. Wilcox, T. R. Siegler, M. Perryman, A. Andrady, R. Narayan and K. L. Law, *Science*, 2015, **347**, 768–771.

5 D. C. Wilson, Global Waste Management Outlook (International Solid Waste Association and United National Environment Programme, 2015).

6 Ellen MacArthur Foundation, *The new plastics economy: rethinking the future of plastics & catalysing action*, 2017.

7 R. Geyer, J. R. Jambeck and K. L. Law, *Sci. Adv.*, 2017, **3**, 1700782.

8 U. S. Environmental Protection Agency, (EPA), Advancing Sustainable Materials Management: 2018 Fact Sheet" (December 2020 version), can be found under **https://www.epa.gov/sites/default/files/2021-01/documents/2018_ff_fact_sheet_dec_2020_fnl_508.pdf**, 2020.

9 IHS Markit, *PET polymer: chemical economics handbook*, 2021, can be found under **https://ihsmarkit.com/products/pet-polymer-chemical-economics-handbook.html**.

10 EEA, EU Recycled 41% of Plastic Packaging Waste in 2019. Available online: **https://ec.europa.eu/eurostat/web/products-eurostat-news/-/ddn-20211027-2**.

11 European Commission, Communication from the Commission to the Council, the European Parliament, the European Economic and Social Committee and the Committee of the Regions: Civil Society Dialogue Between the EU and Candidate Countries, European Commission: Brussels, Belgium, vol. 290, 2005.

12 D. K. A. Barnes, F. Galgani, R. C. Thompson and M. Barlaz, *Philos. Trans. R. Soc. Lond., B*, 2009, **364**, 1985–1998.

13 P. Benyathiar, P. Kumar, G. Carpenter, J. Brace and D. K. Mishra, *Polymers*, 2022, **14**, 2366.

14 G. Ghoshal, *Trends Beverage Packaging*, 2019, vol. 16, pp. 21–50.

15 J. P. Lange, *Energy Environ. Sci.*, 2021, **14**, 4358–4376.

16 J. M. Garcia and M. L. Robertson, *Science*, 2017, **358**, 870–872.

17 A. Rahimi and J. M. García, *Nat. Rev. Chem.*, 2017, **1**, 0046.

18 M. Hong and E. Y. X. Chen, *Green Chem.*, 2017, **19**, 3692–3706.

19 H. Sardon and A. P. Dove, *Science*, 2018, **360**, 380–381.

20 J. C. Worch and A. P. Dove, *ACS Macro Lett.*, 2020, **9**, 1494–1506.

21 Q. Hou, M. Zhen, H. Qian, Y. Nie, X. Bai, T. Xia, M. L. U. Rehman, Q. Li and M. Ju, *Cell Rep. Phys. Sci.*, 2021, **2**, 100514.

22 A. Rahimi and J. M. García, *Nat. Chem. Rev.*, 2017, **1**, 0046.

23 I. A. Ignatyev, W. Thielemans and B. Vander Beke, *ChemSusChem*, 2014, **7**, 1579–1593.

24 D. H. Kim, D. O. Han, K. I. Shim, J. K. Kim, J. G. Pelton, M. H. Ryu, J. C. Joo, J. W. Han, H. T. Kim and K. H. Kim, *ACS Catal.*, 2021, **11**, 3996–4008.

25 Y. Li, M. Wang, X. Liu, C. Hu, D. Xiao and D. Ma, *Angew. Chem., Int. Ed.*, 2022, **61**, e202117205.

26 Z. O. G. Schyns and M. P. Shaver, *Macromol. Rapid Commun.*, 2021, **42**, 2000415.

27 M.-Q. Zhang, M. Wang, B. Sun, C. Hu, D. Xiao and D. Ma, *Chem*, 2022, **8**, 2912–2923.

28 M. Chu, Y. Liu, X. Lou, Q. Zhang and J. Chen, *ACS Catal.*, 2022, **12**, 4659–4679.

29 V. Tournier, C. M. Topham, A. Gilles, B. David, C. Folgoas, E. Moya-Leclair, E. Kamionka, M. L. Desrousseaux, H. Texier, S. Gavalda, M. Cot, E. Guémard, M. Dalibey, J. Nomme, G. Cioci, S. Barbe, M. Chateau, I. André, S. Duquesne and A. Marty, *Nature*, 2020, **580**, 216–219.

30 H. Lu, D. J. Diaz, N. J. Czarnecki, C. Zhu, W. Kim, R. Shroff, D. J. Acosta, B. R. Alexander, H. O. Cole, Y. Zhang, N. A. Lynd, A. D. Ellington and H. S. Alper, *Nature*, 2022, **604**, 662–667.

31 X. Han, W. Liu, J.-W. Huang, J. Ma, Y. Zheng, T.-P. Ko, L. Xu, Y.-S. Cheng, C.-C. Chen and R.-T. Guo, *Nat. Commun.*, 2017, **8**, 2106.

32 S. Javed and D. Vogt, *ACS Sustainable Chem. Eng.*, 2023, **11**, 11541–11547.

33 Z. Fehér, J. Kiss, P. Kisszékelyi, J. Molnár, P. Huszthy, L. Kárpáti and J. Kupai, *Green Chem.*, 2022, **24**, 8447–8459.

34 S. Shirazimoghaddam, I. Amin, J. A. F. Albanese and N. R. Shiju, *ACS Eng. Au*, 2023, **3**, 37–44.

35 N. A. Rorrer, S. Nicholson, A. Carpenter, M. J. Biddy, N. J. Grundl and G. T. Beckham, *Joule*, 2019, **3**, 1006–1027.

36 C. Jehanno, J. Demarteau, D. Mantione, M. C. Arno, F. Ruipérez, J. L. Hedrick, A. P. Dove and H. Sardon, *Angew. Chem., Int. Ed.*, 2021, **60**, 6710–6717.

37 Y. Hu, S. Zhang, J. Xu, Y. Liu, A. Yu, J. Qian and Y. Xie, *Angew. Chem., Int. Ed.*, 2023, e202312564.

38 E. M. Krall, T. W. Klein, R. J. Andersen, A. J. Nett, R. W. Glasgow, D. S. Reader, B. C. Dauphinais, S. P. Mc Ilrath, A. A. Fischer, M. J. Carney, D. J. Hudson and N. J. Robertson, *Chem. Commun.*, 2014, **50**, 4884–4887.

39 S. Westhues, J. Idel and J. Klankermayer, *Sci. Adv.*, 2018, **4**, eaat9669.

40 S. Zhang, Q. Hu, Y.-X. Zhang, H. Guo, Y. Wu, M. Sun, X. Zhu, J. Zhang, S. Gong, P. Liu and Z. Niu, *Nat. Sustainability*, 2023, **6**, 965–973.

41 J. Zhang, G. Leitus, Y. Ben-David and D. Milstein, *Angew. Chem., Int. Ed.*, 2006, **45**, 1113–1115.

42 S. Ügdüler, K. M. Van Geem, R. Denolf, M. Roosen, N. Mys, K. Ragaertc and S. De Meester, *Green Chem.*, 2020, **22**, 5376–5394.

43 Y. Kratish and T. J. Marks, *Angew. Chem., Int. Ed.*, 2022, **61**, e202112576.

44 P. Pereira, E. Savage and C. W. Pester, *ACS Sustainable Chem. Eng.*, 2023, **11**, 7203–7209.

45 S. Zhang, W. Xu, R. Du, X. Zhou, X. Liu, S. Xu and Y. Z. Wang, *Green Chem.*, 2022, **24**, 3284–3292.

46 G. P. Karayannidis, A. P. Chatziavgoustis and D. S. Achilias, *Adv. Polym. Technol.*, 2002, **21**, 250–259.

47 K. Fukushima, J. M. Lecuyer, D. S. Wei, H. W. Horn, G. O. Jones, H. A. Al-Megren, A. M. Alabdulrahman, F. D. Alsewailem, M. A. McNeil, J. E. Rice and J. L. Hedrick, *Polym. Chem.*, 2013, **4**, 1610–1616.

48 K. Ghosal and K. Sarkar, *New J. Chem.*, 2019, **43**, 14166–14178.

49 E. Barnard, J. J. R. Arias and W. Thielemans, *Green Chem.*, 2021, **23**, 3765–3789.

50 W. Yang, G. A. Filonenko and E. A. Pidko, *Chem. Commun.*, 2023, **59**, 1757–1768.

51 Q. Wang, X. Yao, Y. Geng, Q. Zhou, X. Lu and S. Zhang, *Green Chem.*, 2015, **17**, 2473–2479.

52 Y. Liu, X. Yao, H. Yao, Q. Zhou, J. Xin, X. Lu and S. Zhang, *Green Chem.*, 2020, **22**, 3122–3131.

53 A. Bohre, P. R. Jadhao, K. Tripathi, K. K. Pant, B. Likozar and B. Saha, *ChemSusChem*, 2023, **16**, e202300142.

54 M. Wang, Y. Li, L. Zheng, T. Hu, M. Yan and C. Wu, *Polym. Chem.*, 2024, **15**, 585–608.

55 K. Ghosal and C. Nayak, *Mater. Adv.*, 2022, **3**, 1974–1992.

56 L. Bartolome, M. Imran, K. G. Lee, A. Sangalang, J. K. Ahn and D. H. Kim, *Green Chem.*, 2014, **16**, 279–286.

57 F. R. Veregue, C. T. P. da Silva, M. P. Moisés, J. G. Meneguin, M. R. Guilherme, P. A. Arroyo, S. L. Favaro, E. Radovanovic, E. M. Girotto and A. W. Rinaldi, *ACS Sustainable Chem. Eng.*, 2018, **6**, 12017–12024.

58 B. Swapna, N. Singh, S. Patoway, P. Bharali, G. Madras and P. Sudarsanam, *Catal. Sci. Technol.*, 2024, **14**, 5574–5587.

59 E. H. Kim, I. Park, S. H. Kim, J. F. Kim, Y. H. Choi and H. Lee, *Chem. Eng. J.*, 2024, 155865.

60 J.-T. Du, H. Wu, Y. Jie, Y. Xia, Z. Yang, H. Yan, Q. Wang, J.-X. Wang and J.-F. Chen, *Chem. Eng. J.*, 2025, 121042.

61 B. Swapna, S. B. Putla, A. Ramesh, C. Subrahmanyam, G. Madras and P. Sudarsanam, *Sustainable Energy Fuels*, 2024, **8**, 5170–5180.

62 T. Wang, C. Shen, G. Yu and X. Chen, *Fuel*, 2021, **304**, 121397.

63 J. C. Worch and A. P. Dove, *ACS Macro Lett.*, 2020, **9**, 1494–1506.

64 Y. Kratish, J. Li, S. Liu, Y. Gao and T. J. Marks, *Angew. Chem., Int. Ed.*, 2020, **59**, 19857–19861.

65 M. J. Kanga, H. J. Yua, J. Jegala, H. S. Kimb and H. G. Cha, *Chem. Eng. J.*, 2020, 125655.

66 Z. Cao, X. Fu, H. Li, S. Pandit, F. M. A. Noa, L. Öhrström, A. Zelezniak and I. Mijakovic, *ACS Sustainable Chem. Eng.*, 2023, **11**, 15506–15512.

67 R. Hille, C. Schulzke and M. L. Kirk, *Molybdenum and Bioinorganic Tungsten Enzymes*, The Royal Society of Chemistry, UK, 2016, pp. 68–93.

68 P. Salonen, J. A. Schachner, A. Peuronen, M. Lahtinen, F. Belaj, N. C. M. Zanetti and A. Lehtonen, *Mol. Catal.*, 2023, **540**, 113034.

69 Y. Kratish, T. Nakamuro, Y. Liu, J. Li, I. Tomotsuka, K. Harano, E. Nakamura and T. J. Marks, *Bull. Chem. Soc. Jpn.*, 2021, **94**, 427–432.

70 S. L. Wegener, T. J. Marks and P. C. Stair, *Acc. Chem. Res.*, 2012, **45**, 206–214.

71 T. L. Lohr, A. R. Mouat, P. Stair, M. Delferro and T. J. Marks, *Energy Environ. Sci.*, 2017, **10**, 1558–1562.

72 A. R. Mouat, T. L. Lohr, E. C. Wegener, J. T. Miller, M. Delferro, P. C. Stair and T. J. Marks, *ACS Catal.*, 2016, **6**, 6762–6769.

73 R. Taylor, *J. Chem. Soc., Perkin Trans. 2*, 1972, 165–168.

74 F. Neese, *Wiley Interdiscip. Rev.: Comput. Mol. Sci.*, 2012, **2**, 73–78.

75 J. Li, A. Das, Q. Ma, M. J. Bedzyk, Y. Kratish and T. J. Marks, *ACS Catal.*, 2022, **12**, 1247–1257.

76 H. Aoyama, M. Tokunaga, S.-I. Hiraiwa, Y. Shirogane, Y. Obora and Y. Tsuji, *Org. Lett.*, 2004, **6**, 509–512.

77 P. S. Roy, G. Garnier, F. Allais and K. Saito, *ChemSusChem*, 2021, **14**, 4007–4027.

78 Y. Jing, Y. Wang, S. Furukawa, J. Xia, C. Sun, M. J. Hülsey, H. Wang, Y. Guo, X. Liu and N. Yan, *Angew. Chem., Int. Ed.*, 2021, **60**, 5527–5535.

79 K. Nomura, X. Peng, H. Kim, K. Jin, H. J. Kim, A. F. Bratton, C. R. Bond, A. E. Broman, K. M. Miller and C. J. Ellison, *ACS Appl. Mater. Interfaces*, 2020, **12**, 9726–9735.

80 K. P. Sullivan, A. Z. Werner, K. J. Ramirez, L. D. Ellis, J. R. Bussard, B. A. Black, D. G. Brandner, F. Bratti, B. L. Buss, X. Dong, S. J. Haugen, M. A. Ingraham, M. O. Konev, W. E. Michener, J. Miscall, I. Pardo, S. P. Woodworth, A. M. Guss, Y. R. Leshkov, S. S. Stahl and G. T. Beckham, *Science*, 2022, **378**, 207–211.

81 A. Agarwal, Y. Liu, M. Hanazawa, J. Li, T. Nakamuro, E. Nakamura, Y. Kratish and T. J. Marks, *Catal. Sci. Technol.*, 2025, DOI: **10.1039/D4CY01517G**.